HHS Public Access

Author manuscript

Leukemia. Author manuscript; available in PMC 2017 September 07.

Published in final edited form as:

Leukemia. 2017 September ; 31(9): 1962–1974. doi:10.1038/leu.2016.377.

Mass Cytometry Analysis Reveals Hyperactive NF Kappa B Signaling in Myelofibrosis and Secondary Acute Myeloid Leukemia

Daniel A.C. Fisher[1], **Olga Malkova**[2], **Elizabeth K. Engle**[1], **Cathrine Miner**[2], **Mary C. Fulbright**[1], **Gregory K. Behbehani**[3], **Taylor B. Collins**[1], **Shovik Bandyopadhyay**[1], **Amy Zhou**[1], **Garry P. Nolan**[4], and **Stephen T. Oh**[1]

[1]Division of Hematology, Washington University School of Medicine, St. Louis, MO

[2]Center for Human Immunology and Immunotherapy Programs, Washington University School of Medicine, St. Louis, MO

[3]Division of Hematology, Stanford University School of Medicine

[4]Department of Microbiology & Immunology, Stanford University School of Medicine

Abstract

Myeloproliferative neoplasms (MPNs) feature a malignant clone containing the *JAK2* V617F mutation, or another mutation causing dysregulated JAK2 kinase activity. The multiple disease phenotypes of MPNs, and their tendency to transform phenotypically, suggest pathophysiologic heterogeneities beyond a common phenomenon of JAK2 hyperactivation. JAK2 has the potential to activate multiple other signaling molecules, either directly through downstream effectors, or indirectly through induction of target gene expression. We have interrogated myeloproliferative signaling in myelofibrosis (MF) and secondary acute myeloid leukemia (sAML) patient samples using mass cytometry, which allows the quantitative measurement of multiple signaling molecules simultaneously at the single cell level, in cell populations representing a nearly complete spectrum of hematopoiesis. MF and sAML malignant cells demonstrated a high prevalence of hyperactivation of the JAK-STAT, MAP kinase, PI3 kinase, and NFκB signaling pathways. Constitutive NFκB signaling was evident across MF and sAML patients. A supporting GSEA analysis of MF showed many NFκB target genes to be expressed above normal levels in MF patient CD34+ cells. NFκB inhibition suppressed colony formation from MF CD34+ cells. This study indicates that NFκB signaling contributes to human myeloproliferative disease and is abnormally activated in MF and sAML.

Corresponding author: Stephen Oh, M.D., Ph.D., Division of Hematology, Washington University School of Medicine, 660 S. Euclid Ave, Campus Box 8125, St. Louis, MO 63110, Phone: (314) 362-8846, Fax: (314) 362-8826, stoh@dom.wustl.edu.

CONFLICT OF INTEREST

The authors declare no conflict of interest.

Keywords

Myelofibrosis; secondary acute myeloid leukemia; mass cytometry; signal transduction; NFκB (NF kappa B)

INTRODUCTION

Myeloproliferative neoplasms (MPNs) are characterized by a common pathogenic mechanism: hyperactivation of the JAK2 kinase, most frequently as a result of the *JAK2* V617F mutation.[1,2] *JAK2* V617F and other mutations leading to JAK2 hyperactivation are common among polycythemia vera (PV), essential thrombocythemia (ET), and myelofibrosis (MF, either primary or secondary). The phenotypic diversity of MPNs, however, implies other pathogenic mechanisms besides excessive JAK2 activity. While differences between PV and ET have been associated with mutant *JAK2* homozygosity (predominantly in PV, albeit not rare in ET and MF), and with greater IFNγ-STAT1 target gene expression in ET versus PV,[3] the pathogenic mechanisms that distinguish MF and sAML remain poorly understood.

In this study, multiple myeloproliferative intracellular signaling molecules were quantified in MF and sAML patient samples via mass cytometry, a technology that enables the detection of ≥30 metal-tagged antibodies with single cell resolution.[4] This enables quantitative study of signaling abnormalities in a nearly complete spectrum of hematopoietic cell populations.[4–9] Antibody panels were designed to (1) identify immunophenotypic cell populations throughout myeloid differentiation, whose intracellular signaling could be abnormal in MF or sAML, and (2) interrogate myeloproliferative signaling pathways with previously reported abnormalities in other myeloid neoplasms.[10–15]

JAK2 hyperactivation is the known common signaling abnormality underlying PV, ET, and MF.[16–21] It is the primary known consequence of mutations in *JAK2, MPL, SH2B3* (*LNK*), and *CALR*, found in the majority of human MPN clones.[15,21–24] JAK2 signals through its direct substrates STAT3 and STAT5, but can also collaterally activate a number of other signaling pathways: notably, the MAP kinase, PI3 kinase and NFκB signaling pathways (Supplementary Figure S1).[25] This study measures the activities of multiple effectors in these pathways via mass cytometry (Supplementary Table S1). Mutations in genes outside the JAK-STAT pathway, particularly in genes encoding epigenetic factors, are abundant in MF and sAML.[1,25,26] Furthermore, approximately 50% of post-*JAK2* V617F-MPN sAMLs lack the *JAK2* mutation.[27] By implication, these sAMLs are either not driven by JAK2 hyperactivity, or else achieve JAK2 hyperactivity by an alternative mechanism for which mutant JAK2 is dispensable. Therefore JAK2 dysregulation is unlikely to be the only signaling abnormality present in MF and sAML.

NFκB hyperactivation has previously been observed in a subset of *de novo* AMLs,[12,28,29] particularly those of the FLT3-ITD subtype,[13] and in myelodysplastic syndromes.[14] In MF, multiple cytokines are present systemically at supranormal levels, including several that can activate NFκB signaling non-cell-autonomously.[30,31] The present study establishes the widespread prevalence of NFκB hyperactivation in MF and sAML. NFκB hyperactivation in

MF and sAML could occur via both cell autonomous signaling downstream of active JAK2 and non-cell autonomous activation by cytokines.

MATERIALS AND METHODS

Patient samples

Peripheral blood (PB) or bone marrow (BM) samples were obtained with written consent according to a protocol approved by the Washington University Human Studies Committee (WU no. 01-1014). Mononuclear cells (PBMC or BMMC) were obtained by Ficoll gradient extraction and cryopreserved according to standard procedures. Clinical and genetic information for patients studied (16 MF, 10 sAML) is included in Supplementary Table S2. Variant allele frequency (VAF) was obtained for the *JAK2* V617F mutation by quantitative PCR.[32] A total of 12 MF patients (7 *JAK2* V617F-positive) and 10 sAML patients (6 *JAK2* V617F-positive) were included in mass cytometry experiments in this study, with 4 additional MF patients included in colony forming unit (CFU) assays only. Healthy controls for these experiments are listed in Supplementary Table S3.

Targeted gene sequencing

A custom capture panel was designed for targeted sequencing of SNVs (single nucleotide variants) and exons in genes known or predicted to be associated with MPN or AML pathogenesis. The first set of patients was analyzed using a custom capture array from Roche NimbleGen (Madison, WI) with additional capture probes from Integrated DNA Technologies (Coralville, IA) as described previously.[33] Capture probes for additional SNV and exon targets (as listed in Supplementary Table S4) were added for a second round of sequencing. Sequencing was done on the Illumina HiSeq2000 and HiSeq2500 platforms according to the manufacturer's recommendations (Illumina Inc, San Diego, CA). Variant detection and validation was performed as previously described.[33] Potential pathogenic mutations were identified for a subset of patients (Supplementary Table S2).

Cell treatment with cytokines and/or signaling inhibitors

Conditions were derived from prior mass cytometry signaling studies of healthy human bone marrow.[4] Briefly, cryopreserved cells were thawed into RPMI containing 10% fetal bovine serum, heparin (20 U/mL, Sigma, St. Louis, MO), and benzonase (25 mU/mL, Sigma), and labeled with cisplatin (2.5 μM, Enzo Life Sciences, Farmingdale, NY) in serum free RPMI.[34] Cisplatin-treated cells were incubated in serum-containing RPMI for 30 minutes, followed by 1 hour incubation in the presence or absence of inhibitor (5 μM ruxolitinib or 2 μM IKK inhibitor VII), followed by 15 minute stimulation with cytokine and subsequent fixation and staining. Stimulation conditions in the screening experiment (Figure 1) were: basal (unstimulated), ruxolitinib, thrombopoietin (TPO, 50 ng/mL), TPO plus ruxolitinib, granulocyte colony stimulating factor (G-CSF, 20 ng/mL), and sodium pervanadate (125 μM). Subsequent experiments also included 2 μM IKKiVII, TNFα (20 ng/mL), and IKKiVII plus TNFα. Cytokines were obtained from Peprotech (Rocky Hill, NJ), ruxolitinib from Chemie-Tek (Indianapolis, IN), and IKKiVII from EMD Millipore (Billerica, MA). Intracellular TNFα profiling (Figure 6) included secretion inhibitor (brefeldin A/monensin,

Ebioscience, San Diego, CA), and stimulation with phorbol-N-myristyl-acetate (PMA, Invivogen, San Diego, CA) and ionomycin (EMD Millipore).

Mass cytometry

Cell staining for mass cytometry was performed as described previously,[4] using antibody panels described in Supplementary Table S1. Samples for the screening experiment (Figure 1) were mass-channel barcoded, pooled and stained as a single sample, with signals read on a CyTOF1 mass cytometer (DVS/Fluidigm, South San Francisco, CA) using a debarcoder program to identify individual samples.[5,35,36] For later experiments (Figure 2, 4, 5), samples were stained in batches in individual tubes, and readouts were recorded on a CyTOF2 mass cytometer (DVS/Fluidigm). Data were analyzed in Cytobank (cytobank.org), including both conventional cell population gating (Supplementary Figure S2–S4), and cell clustering via SPADE.[9] Gating for subpopulations of HSPC (hematopoietic stem and progenitor cells) is shown in Supplementary Figure S4, emulating gates previously validated by xenotransplantation.[37]

Statistical analysis of mass cytometry signaling data

For statistical analysis of patient sample signaling readouts versus normal controls across multiple experiments (Figure 3), signal medians were normalized to the mean of the median values of the normal controls within the experiment. Thereby deviation beyond the normal range could be identified. Where multiple experiments utilized samples from the same patient sample collection, the sample from the experiment containing the higher average normal basal median for the given signaling antibody readout was selected for statistical analysis, thereby giving a more conservative statistical analysis from the overall dataset (Figure 3) than from any individual experiment. DREMI analysis (Figure 3g, Supplementary Figure S16) was performed as previously described.[38]

Gene set enrichment analysis (GSEA) for MF CD34+ HSPC

GSEA was performed as previously described.[39] Published expression data from MF and healthy control CD34+ cells was downloaded from Gene Expression Omnibus (http://www.ncbi.nlm.nih.gov/geo/, series GSE53482).[40] NFκB target genes were curated from online databases and published literature,[29,41] and divided into three groups corresponding to canonical and AML-related targets, pro-apoptotic targets, and nonspecific targets, which were assessed both individually and combined (Supplementary Table S5).

Plasma cytokine analysis

Peripheral blood plasma collected under standard protocols was stored at −80°C. Concentrations of 30 cytokines/chemokines were analyzed in duplicate using the Meso Scale Discovery platform with the V-PLEX human cytokine 30-plex kit (Meso Scale Discovery, Rockville, MD).

Colony forming unit (CFU) assays

CFU assays were performed in semisolid culture using Methocult H4035 (StemCell Technologies, Vancouver, BC, Canada), containing G-CSF, GM-CSF, IL-3, SCF, and

supplemented with TPO (10 ng/mL). Lineage-negative (Lin−) CD34+ cells were sorted from normal control BM or MF patient PB (see Supplementary Table S1, S2 for individual patient information; Supplementary Figure S5 for gating) and cultured in Methocult H4035, with or without ruxolitinib, IKKiVII, and/or TNFα, as described in Figure 8.

RESULTS

Dysregulated myeloproliferative signaling across early myeloid differentiation

In an initial screening experiment, bone marrow mononuclear cells (BMMC) from three healthy controls and four MF patients, plus peripheral blood mononuclear cells (PBMC) from five sAML patients were analyzed by mass cytometry (Supplementary Table S2, S3). Samples were stained with antibodies labeling 13 cell surface markers and 17 markers of intracellular signaling, cell division, or apoptosis (Supplementary Table S1). Signaling was analyzed in live, non-apoptotic PBMC/BMMC utilizing the SPADE (Spanning tree Progression of Density normalized Events) clustering algorithm,[9] or by conventional gating (Supplementary Figure S2–S4).

Abnormally elevated levels of the direct JAK2 targets STAT3 and STAT5 were observed in hematopoietic stem and progenitor cells (HSPC) from individual MF or sAML patients, including both *JAK2* mutant and *JAK2* wild-type patients. (Figure 1a–c, Supplementary Figure S6–S9). Elevated STAT phosphorylation could be observed either in the basal (unstimulated) state or in response to cytokines (TPO, G-CSF). In addition, supranormal basal and/or cytokine-induced phosphorylation of ERK, CREB, and/or S6 was observed in MF and sAML HSPC. Increased total IκBα levels were observed in unstimulated HSPC, myeloblasts, B and T cells (Supplementary Figure S10). In contrast to cytokine hypersensitivity of STAT5 phosphorylation, constitutively high IκBα levels generally showed little to no reduction after 1-hour incubation with the JAK inhibitor ruxolitinib (Figure 1d, Supplementary Figure S11).

Based on gating derived from xenotransplant studies,[37,42] HSPC could be subdivided into immunophenotypic cell populations representing myeloid differentiation from a hematopoietic stem cell (HSC)-enriched population (CD34+, CD38−, CD90+, CD45RA−), to lineage-committed blasts (Supplementary Figure S3, S4). Abnormal constitutive signals in MF and sAML patients frequently spanned this entire spectrum of myeloid differentiation (Figure 1e, Supplementary Figure S12).

NFκB hyperactivity in MF and sAML HSPC

Constitutively elevated IκBα levels suggested the hypothesis that the NFκB pathway is dysregulated in MF and sAML. Therefore, a direct measure of NFκB activation, phosphorylated NFκB subunit p65/RELA, was included in all subsequent experiments. Signaling was measured basally and in the presence of tumor necrosis factor (TNFα) and/or the IκB kinase inhibitor IKKiVII, to stimulate or inhibit the NFκB pathway, respectively. In experiments on primary patient samples and controls, phosphorylation of S529 of p65/RELA was utilized as the measure of NFκB activation (Supplementary Table S1). Experiments using the *JAK2* V617F mutant human erythroleukemia (HEL) cell line

demonstrated cooperativity and interdependence between p65/RELA phosphorylation on S529 by Casein Kinase II and phosphorylation on S536 by IκB kinases (Supplementary Figure S13). The p-S529 antibody was preferred in patient samples due to more robust signal in response to TNFα, and potential competition between the two antibodies for a limited pool of activated p65/RELA (data not shown).

Supranormal levels of phosphorylated p65/RELA were observed in unstimulated HSPC (9/12 MF and 6/8 sAML above normal range; Figure 2a, 2b, 3a). In addition, stimulation with TNFα induced p65/RELA phosphorylation above levels observed in healthy controls (4/12 MF patients, 6/8 sAML; Figure 2a, 2b, 3b). Therefore the NFκB pathway was both constitutively active and hypersensitive in patients' HSPC. One hour incubation with IKKiVII inhibited both basal and TNFα stimulated p65/RELA phosphorylation, while a similar incubation with ruxolitinib did not (Figure 2a, 2b; Supplementary Figure S13, S14). Longer ruxolitinib incubations of up to 12 hours produced only minor inhibition of basally elevated p65/RELA phosphorylation, as compared with synchronous incubation without ruxolitinib (Supplementary Figure S15). Patients with elevated basal p65/RELA phosphorylation invariably exhibited this abnormality throughout the spectrum of myeloid differentiation (Figure 2c).

MF HSPC exhibited higher basal phosphorylation of p65/RELA NFκB (in 9/12 patients), compared with the normal bone marrow control population (Figure 3a). The majority of sAML patients (6/8) also exhibited basally elevated phosphorylation of p65/RELA in HSPC, with significant differences observed between MF and sAML patient populations and controls. The highest levels were observed in *JAK2* V617F mutant MF patients, being significantly higher than levels observed in *JAK2* wild-type MF patients, which were also significantly higher than normal controls. TNFα-stimulated p65/RELA phosphorylation was not significantly different in the overall MF patient population versus controls (Figure 3b), although several patients (4/12 MF patients, 6/8 sAML) exhibited a much greater positive deviation from the average experiment-matched control than did any normal control. sAML patients overall and *JAK2* V617F mutant sAML patients specifically showed significant elevation of TNFα stimulated p65/RELA phosphorylation. Basal IκBα, while substantially elevated in several individual patients (3/16 MF and 1/10 sAML patients above the normal range observed in all experiments, Figure 3c; in contrast to 2/4 MF and 3/5 sAML above the normal range observed in the screening experiment, Figure 1a, e), was not significantly elevated in the overall patient populations (Figure 3c).

Basal and TPO-stimulated STAT5 phosphorylation values were substantially above the normal control range in several individual patients (basal: 4/16 MF and 2/10 sAML above normal range; TPO-simulated: 5/16 MF and 3/10 sAML above normal range), but these elevations fell short of statistical significance in all populations except *JAK2* wild-type MF (Figure 3d,e). *JAK2* wild-type sAML patients exhibited significantly lower TPO-stimulated pSTAT5 values than normal controls (Figure 3e), hinting at possible negative feedback on TPO-stimulated JAK2 activation by an active downstream signal. The overlapping ranges of patient versus control pSTAT5 values may reflect more rapid turnover of STAT5 phosphorylation as compared to p65/RELA phosphorylation, thus minimizing basal levels,

and/or potentially the use of a response-saturating dose of activating cytokine (based on responses derived from normal bone marrow[4]).

While NFκB activation parameters did not differ by allele burden in *JAK2* mutant patients (not shown), there was a significant correlation both among MF patients and in the combined MF plus sAML patient group between median basal p-p65/RELA and pSTAT5 levels (Figure 3f). At the single cell level within individual patients, the DREMI (Density Resampled Estimate of Mutual Information)[38] conditional probability algorithm was used to estimate the relative difference in predictive value of cellular pSTAT5 on cellular p-p65/RELA. DREMI scores for patient samples, estimating the relative predictive value of pSTAT5 on p-p65/RELA, were significantly higher in MF and sAML patient sets than normal controls (Figure 3g, Supplementary Figure S16).

Phosphorylation of p38, a MAP kinase pathway target, which can also be activated by TNFα, was significantly elevated in MF HSPC versus both controls and sAML HSPC (Figure 3h). Phosphorylation of CREB, a MAP kinase pathway target, which can be activated downstream of JAK2 (Supplementary Figure S1), was elevated in MF patient HSPC both basally and in response to TPO (Supplementary Figure S18).

Elevated p-p65/RELA in MF and sAML was observed not only in HSPC, but also in other hematopoietic cell populations (Figure 4; similar to IκBα, Supplementary Figure S10, contrast with pCREB, Supplementary Figure S18). T cells showed significant elevation of basal p-p65/RELA in both MF and sAML, as well as significantly higher levels in *JAK2* V617F mutant versus *JAK2* wild-type MF (Figure 4c). Elevation of basal p-p65/RELA in B cells and monocytes was observed in both MF and sAML samples, but was more prevalent in sAML, while hypersensitivity of monocytes to TNFα appeared specific to sAML (Figure 4d–f). Activation of p65/RELA phosphorylation by TNFα, however, was confined to HSPC and monocytes, in patient and control samples (Figure 5b; Supplementary Figure S19–S21).

MF and sAML patients studied by mass cytometry exhibited elevated plasma levels of TNFα (Figure 5c), suggesting that NFκB hyperactivation may be in part non-cell-autonomous, driven by TNFα. To explore this possibility, TNFα expression was examined by mass cytometry in MF patient samples (Figure 6). AML HSPC have been reported to express TNFα, which can activate NFκB non-cell-autonomously.[29] In MF as well as normal control blood, TNFα expression was principally observed in monocytes (Figure 6a). Both monocytes and Lin−CD34+ HSPC, however, exhibited higher TNFα expression than normal controls, both basally and in response to non-specific stimulation with PMA + ionomycin (Figure 6b–d). These findings indicate the potential for NFκB hyperactivation in HSPC to be induced non-cell-autonomously by TNFα. To test the potential role of *JAK2* V617F in TNFα overproduction, TNFα levels in supernatants from BaF3/MPL cells retrovirally expressing empty vector, wild-type *JAK2*, or *JAK2* V617F, were measured (Figure 6e). BaF3/MPL cells expressing *JAK2* V617F produced significantly more TNFα than cells expressing empty vector or wild-type *JAK2.*

Aberrant NFκB pathway target gene expression in MF

Recent studies have profiled gene expression in MF HSPC and granulocytes.[21,40,43] We utilized several published NFκB target gene sets[29,41] to construct a tiered gene list for querying expression data for an NFκB target enrichment profile in MF (Supplementary Table S5). The Tier 1 list comprised well-established NFκB target genes, particularly those observed to be upregulated in AML subtypes.[29,41,44–47] This set was subdivided into Tier 1a, excluding pro-apoptotic gene targets associated with TNFα-FAS activation, and Tier 1b, which constituted pro-apoptotic NFκB target genes. Tier 2 included established but non-specific NFκB target genes, which are also known expression targets of other signaling pathways. Using these categories, a published dataset of gene expression in CD34+ cells from MF patients versus normal controls[40] was queried.

In MF patient (n=42) versus normal bone marrow (n=15) CD34+ cells, there was a trend toward greater expression of NFκB target genes, particularly the more specific Tier 1 gene set (FDR q=0.084, FWER p=0.041; Figure 7a). Both pro-apoptotic (Tier 1b) and non-pro-apoptotic (Tier 1a) NFκB target genes were overexpressed in MF versus normal CD34+ cells (Figure 7a; Supplementary Table S6). A few NFκB target genes were, contrarily, downregulated in MF versus normal CD34+ cells (Figure 7b); however, these did not coincide with the pro-apoptotic Tier 1b genes (Figure 7a). *JAK2* mutant MF patients (n=23) showed stronger enrichment versus controls (n=15) of the Tier 1 gene set (FDR q=0.078; FWER p=0.039) than did *JAK2* wild-type patients (n=19; FDR q=0.17; FWER p=0.083; Supplementary Figure S22; Supplementary Table S6). The pro-apoptotic Tier 1b gene set was particularly enriched in the *JAK2* mutant MF patients versus controls (FDR q=0.029; FWER p=0.015 Supplementary Figure S22; Supplementary Table S6) and versus *JAK2* wild-type patients (FDR q=0.048; FWER p=0.024; Figure 7c; Supplementary Table S6). In contrast, non-pro-apoptotic Tier 1a NFκB target genes were not clearly enriched in *JAK2* mutant versus *JAK2* wild-type MF patients (Figure 7c; Supplementary Table S6). The less specific Tier 2 and the combined Tier 1+2 gene sets were also significantly enriched in *JAK2* mutant versus wild-type patients (Supplementary Table S6; Supplementary Figure S22). Overall, the majority of NFκB target genes were overexpressed in CD34+ cells from all MF patients versus controls; however, enrichment of pro-apoptotic NFκB target genes was most pronounced in *JAK2* mutant MF patients.

NFκB pathway inhibition reduces myeloid colony formation

To assess the contribution of NFκB activity to myeloproliferation, cell growth and colony formation assays were performed using IKKiVII alone or in combination with ruxolitinib. Growth of *JAK2* V617F mutant HEL cells was inhibited by either IKKiVII or ruxolitinib, and the combination of IKKiVII plus ruxolitinib produced enhanced inhibition (Supplementary Figure S23). In colony forming assays, IKKiVII inhibited colony formation from MF patient CD34+ cells similarly to ruxolitinib, and the combination of IKKiVII and ruxolitinib produced a combinatorial inhibitory effect (Figure 8a; Supplementary Figure S24). Colony numbers were also reduced in the presence of TNFα; however, colony formation was almost entirely eliminated by IKKiVII and/or ruxolitinib in the presence of TNFα. Similar inhibitory effects of IKKiVII and/or ruxolitinib were observed on normal CD34+ cells (Figure 8b). However, individual MF patients with pronounced NFκB

hyperactivition (**MF9, MF10, MF16: See** Figure 2c; Supplementary Figure S20) were those with the strongest inhibitory responses to IKKiVII and/or TNFα (Figure 8a, Supplementary Figure S24a).

DISCUSSION

Intracellular flow cytometry has been used previously to identify and describe signaling dysregulations in hematopoietic cancers.[10,11,15,48,49] We have extended this approach to MF and sAML using mass cytometry, based on the hypothesis that MF and sAML likely possess intracellular signaling phenotypes beyond the canonical JAK-STAT pathway. Indeed, the NFκB, MAP kinase, and PI3 kinase pathways, as well as the JAK-STAT pathway, exhibited constitutive signal activation and hypersensitivity to cytokine stimulation. Among these pathways, the NFκB pathway showed the greatest statistical deviation from normal over the MF and sAML patient groups studied. While measures of NFκB hyperactivation appeared most pronounced in *JAK2* V617F mutant MF, NFκB hyperactivation was also evident in both *JAK2* mutant and non-mutant MF and sAML. Consistent with this evidence, increased expression of NFκB pathway target genes was identified in an independently published MF gene expression dataset,[40] in both *JAK2* mutant and non-mutant MF patients. Elevated plasma TNFα levels were observed in almost all of the patients examined, consistent with previous studies on MF patients.[30,31] Data from colony-forming unit (CFU) assays suggest that NFκB activity is essential for myeloproliferation both normally and in MF. Therefore we hypothesize that NFκB activity is an intrinsic component of myeloproliferation, which is heightened in MF and sAML.

NFκB pathway hyperactivation is a novel finding in MPNs and sAML, although it has previously been reported in a subset of *de novo* AMLs, including but not exclusively the *FLT-3* ITD subtype,[12,13,28,29] and in myelodysplastic syndromes.[14] *JAK2*-mutant MPN and *FLT-3* ITD AML have in common an activating kinase mutation in the malignant clone, which may be a cause of NFκB hyperactivation. Consistent with this notion, correlation between STAT5 and p65/RELA phosphorylation was observed in MF and sAML.

An activating kinase mutation can lead to NFκB pathway activation by two basic mechanisms: cell autonomously from signaling downstream of the mutant kinase, or non-cell autonomously from upregulated expression of an activating ligand, such as TNFα (Supplementary Figure S1). Both of these processes may be occurring simultaneously in MF and sAML. IKK1 and p65/RELA are substrates of activating phosphorylation by AKT, S6K, and PIM kinases, which can be upregulated or activated downstream of activated JAK2 (Supplementary Figure S1).[50,51] Likewise, circulating levels of multiple cytokines, including TNFα, are elevated in MF.[30,31] Recent studies have shown positive feedback between TNFα and NFκB in AML mouse models, with a combination of pro- and anti-apoptotic signaling activated by TNFα.[29,52] Notably, mutations in NFκB pathway genes, while recurrent in several lymphoid neoplasms, appear very rare in myeloid neoplasms.[53,54]

This study illustrates the potential for mass cytometry to identify intracellular signaling phenotypes in cancer. NFκB hyperactivation in MF and sAML was observed throughout early myeloid development, including immunophenotypic HSC, the population expected to

maintain a chronic MPN over a period of years and/or transform to sAML.[27,55] Evidence of chronic NFκB activation was also identified in T and B cells, in spite of these frequently not being part of the malignant clone.[55] This suggests a cytokine-mediated, non-cell autonomous component to the NFκB phenotype, which is consistent with the hypothesis that TNFα contributes to malignant clonal dominance in MF[31] and AML.[29,52]

In conclusion, NFκB hyperactivation is widespread in both MF and sAML, both with and without mutation of *JAK2*. NFκB hyperactivation, and other signaling dysregulations observed, must be considered significant signaling phenotypes in these diseases, which may be important contributors to their pathophysiology. The presence of these signaling phenotypes in HSPC, including phenotypic HSC, suggests potential roles in the development or maintenance of clonal dominance. Alternatively, the NFκB pathway, containing pro-apoptotic and anti-apoptotic components, may protect the malignant clone from pro-apoptotic signals induced by cytokines, to which both malignant and residual non-malignant cells are exposed. Further studies will be needed to elucidate the therapeutic potential of NFκB pathway inhibition in myeloid neoplasms.

Supplementary Material

Refer to Web version on PubMed Central for supplementary material.

Acknowledgments

This work was supported by NIH grants K08HL106576 (Oh), K12HL087107 (Oh), and T32HL007088 (Engle, Fisher). This research was also supported by an American Cancer Society Postdoctoral Fellowship (Fisher). This work was also supported by a Doris Duke-Damon Runyon Clinical Investigator Award (Oh), BRIGHT Institute Pilot Research Project Award (Oh), Burroughs Wellcome Fund Collaborative Research Travel Grant (Oh), Sidney Kimmel Scholar Award (Oh), Leukemia Research Foundation New Investigator Award (Oh), and American Cancer Society Institutional Research Grant (Oh). Additional support was provided by the Washington University Institute of Clinical and Translational Sciences grant UL1TR000448 from the National Center for Advancing Translational Sciences of NIH. Support for patient sample collection and processing was provided by NIH grant P01CA101937. These studies were supported in part by funding provided by Incyte Corporation. Technical support was provided by the Alvin J. Siteman Cancer Center Tissue Procurement Core Facility, Flow Cytometry Core, and Immunomonitoring Laboratory, which are supported by NCI Cancer Center Support Grant P30CA91842. The Immunomonitoring Laboratory is also supported by the Center for Human Immunology and Immunotherapy Programs. The authors thanks C. Miner for assistance with mass cytometry experiments, D. Moore and K. Luber for assistance with clinical samples and data, and D. Bender and C. Wilson for assistance with cytokine assays.

References

1. Hobbs GS, Rampal RK. Clinical and molecular genetic characterization of myelofibrosis. Current opinion in hematology. 2015; 22(2):177–83. [PubMed: 25635755]
2. Viny AD, Levine RL. Genetics of myeloproliferative neoplasms. Cancer journal. 2014; 20(1):61–5.
3. Chen E, Beer PA, Godfrey AL, Ortmann CA, Li J, Costa-Pereira AP, et al. Distinct clinical phenotypes associated with JAK2V617F reflect differential STAT1 signaling. Cancer cell. 2010; 18(5):524–35. [PubMed: 21074499]
4. Bendall SC, Simonds EF, Qiu P, Amir el AD, Krutzik PO, Finck R, et al. Single-cell mass cytometry of differential immune and drug responses across a human hematopoietic continuum. Science. 2011; 332(6030):687–96. [PubMed: 21551058]
5. Bodenmiller B, Zunder ER, Finck R, Chen TJ, Savig ES, Bruggner RV, et al. Multiplexed mass cytometry profiling of cellular states perturbed by small-molecule regulators. Nature biotechnology. 2012; 30(9):858–67.

6. Amir el AD, Davis KL, Tadmor MD, Simonds EF, Levine JH, Bendall SC, et al. viSNE enables visualization of high dimensional single-cell data and reveals phenotypic heterogeneity of leukemia. Nature biotechnology. 2013; 31(6):545–52.
7. Behbehani GK, Samusik N, Bjornson ZB, Fantl WJ, Medeiros BC, Nolan GP. Mass Cytometric Functional Profiling of Acute Myeloid Leukemia Defines Cell-Cycle and Immunophenotypic Properties That Correlate with Known Responses to Therapy. Cancer Discov. 2015; 5(9):988–1003. [PubMed: 26091827]
8. Levine JH, Simonds EF, Bendall SC, Davis KL, Amir el AD, Tadmor MD, et al. Data-Driven Phenotypic Dissection of AML Reveals Progenitor-like Cells that Correlate with Prognosis. Cell. 2015; 162(1):184–97. [PubMed: 26095251]
9. Qiu P, Simonds EF, Bendall SC, Gibbs KD Jr, Bruggner RV, Linderman MD, et al. Extracting a cellular hierarchy from high-dimensional cytometry data with SPADE. Nature biotechnology. 2011; 29(10):886–91.
10. Irish JM, Hovland R, Krutzik PO, Perez OD, Bruserud O, Gjertsen BT, et al. Single cell profiling of potentiated phospho-protein networks in cancer cells. Cell. 2004; 118(2):217–28. [PubMed: 15260991]
11. Kotecha N, Flores NJ, Irish JM, Simonds EF, Sakai DS, Archambeault S, et al. Single-cell profiling identifies aberrant STAT5 activation in myeloid malignancies with specific clinical and biologic correlates. Cancer cell. 2008; 14(4):335–43. [PubMed: 18835035]
12. Guzman ML, Neering SJ, Upchurch D, Grimes B, Howard DS, Rizzieri DA, et al. Nuclear factor-kappaB is constitutively activated in primitive human acute myelogenous leukemia cells. Blood. 2001; 98(8):2301–7. [PubMed: 11588023]
13. Grosjean-Raillard J, Ades L, Boehrer S, Tailler M, Fabre C, Braun T, et al. Flt3 receptor inhibition reduces constitutive NFkappaB activation in high-risk myelodysplastic syndrome and acute myeloid leukemia. Apoptosis : an international journal on programmed cell death. 2008; 13(9): 1148–61. [PubMed: 18670883]
14. Grosjean-Raillard J, Tailler M, Ades L, Perfettini JL, Fabre C, Braun T, et al. ATM mediates constitutive NF-kappaB activation in high-risk myelodysplastic syndrome and acute myeloid leukemia. Oncogene. 2009; 28(8):1099–109. [PubMed: 19079347]
15. Oh ST, Simonds EF, Jones C, Hale MB, Goltsev Y, Gibbs KD Jr, et al. Novel mutations in the inhibitory adaptor protein LNK drive JAK-STAT signaling in patients with myeloproliferative neoplasms. Blood. 2010; 116(6):988–92. [PubMed: 20404132]
16. Baxter EJ, Scott LM, Campbell PJ, East C, Fourouclas N, Swanton S, et al. Acquired mutation of the tyrosine kinase JAK2 in human myeloproliferative disorders. Lancet. 2005; 365(9464):1054–61. [PubMed: 15781101]
17. James C, Ugo V, Le Couedic JP, Staerk J, Delhommeau F, Lacout C, et al. A unique clonal JAK2 mutation leading to constitutive signalling causes polycythaemia vera. Nature. 2005; 434(7037): 1144–8. [PubMed: 15793561]
18. Kralovics R, Passamonti F, Buser AS, Teo SS, Tiedt R, Passweg JR, et al. A gain-of-function mutation of JAK2 in myeloproliferative disorders. The New England journal of medicine. 2005; 352(17):1779–90. [PubMed: 15858187]
19. Levine RL, Wadleigh M, Cools J, Ebert BL, Wernig G, Huntly BJ, et al. Activating mutation in the tyrosine kinase JAK2 in polycythemia vera, essential thrombocythemia, and myeloid metaplasia with myelofibrosis. Cancer cell. 2005; 7(4):387–97. [PubMed: 15837627]
20. Schwemmers S, Will B, Waller CF, Abdulkarim K, Johansson P, Andreasson B, et al. JAK2V617F-negative ET patients do not display constitutively active JAK/STAT signaling. Experimental hematology. 2007; 35(11):1695–703. [PubMed: 17764814]
21. Rampal R, Al-Shahrour F, Abdel-Wahab O, Patel JP, Brunel JP, Mermel CH, et al. Integrated genomic analysis illustrates the central role of JAK-STAT pathway activation in myeloproliferative neoplasm pathogenesis. Blood. 2014; 123(22):e123–33. [PubMed: 24740812]
22. Klampfl T, Gisslinger H, Harutyunyan AS, Nivarthi H, Rumi E, Milosevic JD, et al. Somatic mutations of calreticulin in myeloproliferative neoplasms. The New England journal of medicine. 2013; 369(25):2379–90. [PubMed: 24325356]

23. Nangalia J, Massie CE, Baxter EJ, Nice FL, Gundem G, Wedge DC, et al. Somatic CALR mutations in myeloproliferative neoplasms with nonmutated JAK2. The New England journal of medicine. 2013; 369(25):2391–405. [PubMed: 24325359]
24. Elf S, Abdelfattah NS, Chen E, Perales-Paton J, Rosen EA, Ko A, et al. Mutant Calreticulin Requires Both Its Mutant C-terminus and the Thrombopoietin Receptor for Oncogenic Transformation. Cancer Discov. 2016; 6(4):368–81. [PubMed: 26951227]
25. Reuther GW. Recurring mutations in myeloproliferative neoplasms alter epigenetic regulation of gene expression. American journal of cancer research. 2011; 1(6):752–62. [PubMed: 22016825]
26. Abdel-Wahab O, Levine RL. Mutations in epigenetic modifiers in the pathogenesis and therapy of acute myeloid leukemia. Blood. 2013; 121(18):3563–72. [PubMed: 23640996]
27. Theocharides A, Boissinot M, Girodon F, Garand R, Teo SS, Lippert E, et al. Leukemic blasts in transformed JAK2-V617F-positive myeloproliferative disorders are frequently negative for the JAK2-V617F mutation. Blood. 2007; 110(1):375–9. [PubMed: 17363731]
28. Figueroa ME, Lugthart S, Li Y, Erpelinck-Verschueren C, Deng X, Christos PJ, et al. DNA methylation signatures identify biologically distinct subtypes in acute myeloid leukemia. Cancer cell. 2010; 17(1):13–27. [PubMed: 20060365]
29. Kagoya Y, Yoshimi A, Kataoka K, Nakagawa M, Kumano K, Arai S, et al. Positive feedback between NF-kappaB and TNF-alpha promotes leukemia-initiating cell capacity. The Journal of clinical investigation. 2014; 124(2):528–42. [PubMed: 24382349]
30. Tefferi A, Vaidya R, Caramazza D, Finke C, Lasho T, Pardanani A. Circulating interleukin (IL)-8, IL-2R, IL-12, and IL-15 levels are independently prognostic in primary myelofibrosis: a comprehensive cytokine profiling study. Journal of clinical oncology : official journal of the American Society of Clinical Oncology. 2011; 29(10):1356–63. [PubMed: 21300928]
31. Fleischman AG, Aichberger KJ, Luty SB, Bumm TG, Petersen CL, Doratotaj S, et al. TNFalpha facilitates clonal expansion of JAK2V617F positive cells in myeloproliferative neoplasms. Blood. 2011; 118(24):6392–8. [PubMed: 21860020]
32. Levine RL, Belisle C, Wadleigh M, Zahrieh D, Lee S, Chagnon P, et al. X-inactivation-based clonality analysis and quantitative JAK2V617F assessment reveal a strong association between clonality and JAK2V617F in PV but not ET/MMM, and identifies a subset of JAK2V617F-negative ET and MMM patients with clonal hematopoiesis. Blood. 2006; 107(10):4139–41. [PubMed: 16434490]
33. Engle EK, Fisher DA, Miller CA, McLellan MD, Fulton RS, Moore DM, et al. Clonal evolution revealed by whole genome sequencing in a case of primary myelofibrosis transformed to secondary acute myeloid leukemia. Leukemia. 2015; 29(4):869–76. [PubMed: 25252869]
34. Fienberg HG, Simonds EF, Fantl WJ, Nolan GP, Bodenmiller B. A platinum-based covalent viability reagent for single-cell mass cytometry. Cytometry Part A : the journal of the International Society for Analytical Cytology. 2012; 81(6):467–75. [PubMed: 22577098]
35. Zunder ER, Finck R, Behbehani GK, Amir el AD, Krishnaswamy S, Gonzalez VD, et al. Palladium-based mass tag cell barcoding with a doublet-filtering scheme and single-cell deconvolution algorithm. Nat Protoc. 2015; 10(2):316–33. [PubMed: 25612231]
36. Behbehani GK, Thom C, Zunder ER, Finck R, Gaudilliere B, Fragiadakis GK, et al. Transient partial permeabilization with saponin enables cellular barcoding prior to surface marker staining. Cytometry Part A : the journal of the International Society for Analytical Cytology. 2014; 85(12): 1011–9. [PubMed: 25274027]
37. Majeti R, Park CY, Weissman IL. Identification of a hierarchy of multipotent hematopoietic progenitors in human cord blood. Cell stem cell. 2007; 1(6):635–45. [PubMed: 18371405]
38. Krishnaswamy S, Spitzer MH, Mingueneau M, Bendall SC, Litvin O, Stone E, et al. Systems biology. Conditional density-based analysis of T cell signaling in single-cell data. Science. 2014; 346(6213):1250689. [PubMed: 25342659]
39. Subramanian A, Tamayo P, Mootha VK, Mukherjee S, Ebert BL, Gillette MA, et al. Gene set enrichment analysis: a knowledge-based approach for interpreting genome-wide expression profiles. Proceedings of the National Academy of Sciences of the United States of America. 2005; 102(43):15545–50. [PubMed: 16199517]

40. Norfo R, Zini R, Pennucci V, Bianchi E, Salati S, Guglielmelli P, et al. miRNA-mRNA integrative analysis in primary myelofibrosis CD34+ cells: role of miR-155/JARID2 axis in abnormal megakaryopoiesis. Blood. 2014; 124(13):e21–32. [PubMed: 25097177]
41. Kuo HP, Wang Z, Lee DF, Iwasaki M, Duque-Afonso J, Wong SH, et al. Epigenetic roles of MLL oncoproteins are dependent on NF-kappaB. Cancer cell. 2013; 24(4):423–37. [PubMed: 24054986]
42. Gibbs KD Jr, Gilbert PM, Sachs K, Zhao F, Blau HM, Weissman IL, et al. Single-cell phospho-specific flow cytometric analysis demonstrates biochemical and functional heterogeneity in human hematopoietic stem and progenitor compartments. Blood. 2011; 117(16):4226–33. [PubMed: 21357764]
43. Guglielmelli P, Zini R, Bogani C, Salati S, Pancrazzi A, Bianchi E, et al. Molecular profiling of CD34+ cells in idiopathic myelofibrosis identifies a set of disease-associated genes and reveals the clinical significance of Wilms' tumor gene 1 (WT1). Stem cells. 2007; 25(1):165–73. [PubMed: 16990584]
44. Bosman MC, Schuringa JJ, Quax WJ, Vellenga E. Bortezomib sensitivity of acute myeloid leukemia CD34(+) cells can be enhanced by targeting the persisting activity of NF-kappaB and the accumulation of MCL-1. Experimental hematology. 2013; 41(6):530–8. e1. [PubMed: 23416210]
45. Hariri F, Arguello M, Volpon L, Culjkovic-Kraljacic B, Nielsen TH, Hiscott J, et al. The eukaryotic translation initiation factor eIF4E is a direct transcriptional target of NF-kappaB and is aberrantly regulated in acute myeloid leukemia. Leukemia. 2013; 27(10):2047–55. [PubMed: 23467026]
46. Wang X, Zhu K, Li S, Liao Y, Du R, Zhang X, et al. MLL1, a H3K4 methyltransferase, regulates the TNFalpha-stimulated activation of genes downstream of NF-kappaB. Journal of cell science. 2012; 125(Pt 17):4058–66. [PubMed: 22623725]
47. Gleixner KV, Ferenc V, Peter B, Gruze A, Meyer RA, Hadzijusufovic E, et al. Polo-like kinase 1 (Plk1) as a novel drug target in chronic myeloid leukemia: overriding imatinib resistance with the Plk1 inhibitor BI 2536. Cancer research. 2010; 70(4):1513–23. [PubMed: 20145140]
48. Irish JM, Anensen N, Hovland R, Skavland J, Borresen-Dale AL, Bruserud O, et al. Flt3 Y591 duplication and Bcl-2 overexpression are detected in acute myeloid leukemia cells with high levels of phosphorylated wild-type p53. Blood. 2007; 109(6):2589–96. [PubMed: 17105820]
49. Irish JM, Myklebust JH, Alizadeh AA, Houot R, Sharman JP, Czerwinski DK, et al. B-cell signaling networks reveal a negative prognostic human lymphoma cell subset that emerges during tumor progression. Proceedings of the National Academy of Sciences of the United States of America. 2010; 107(29):12747–54. [PubMed: 20543139]
50. Neumann M, Naumann M. Beyond IkappaBs: alternative regulation of NF-kappaB activity. FASEB journal : official publication of the Federation of American Societies for Experimental Biology. 2007; 21(11):2642–54. [PubMed: 17431096]
51. Nihira K, Ando Y, Yamaguchi T, Kagami Y, Miki Y, Yoshida K. Pim-1 controls NF-kappaB signalling by stabilizing RelA/p65. Cell death and differentiation. 2010; 17(4):689–98. [PubMed: 19911008]
52. Volk A, Li J, Xin J, You D, Zhang J, Liu X, et al. Co-inhibition of NF-kappaB and JNK is synergistic in TNF-expressing human AML. The Journal of experimental medicine. 2014; 211(6): 1093–108. [PubMed: 24842373]
53. Rossi D, Ciardullo C, Gaidano G. Genetic aberrations of signaling pathways in lymphomagenesis: revelations from next generation sequencing studies. Seminars in cancer biology. 2013; 23(6):422–30. [PubMed: 23665546]
54. Welch JS, Ley TJ, Link DC, Miller CA, Larson DE, Koboldt DC, et al. The origin and evolution of mutations in acute myeloid leukemia. Cell. 2012; 150(2):264–78. [PubMed: 22817890]
55. Delhommeau F, Dupont S, Tonetti C, Masse A, Godin I, Le Couedic JP, et al. Evidence that the JAK2 G1849T (V617F) mutation occurs in a lymphomyeloid progenitor in polycythemia vera and idiopathic myelofibrosis. Blood. 2007; 109(1):71–7. [PubMed: 16954506]

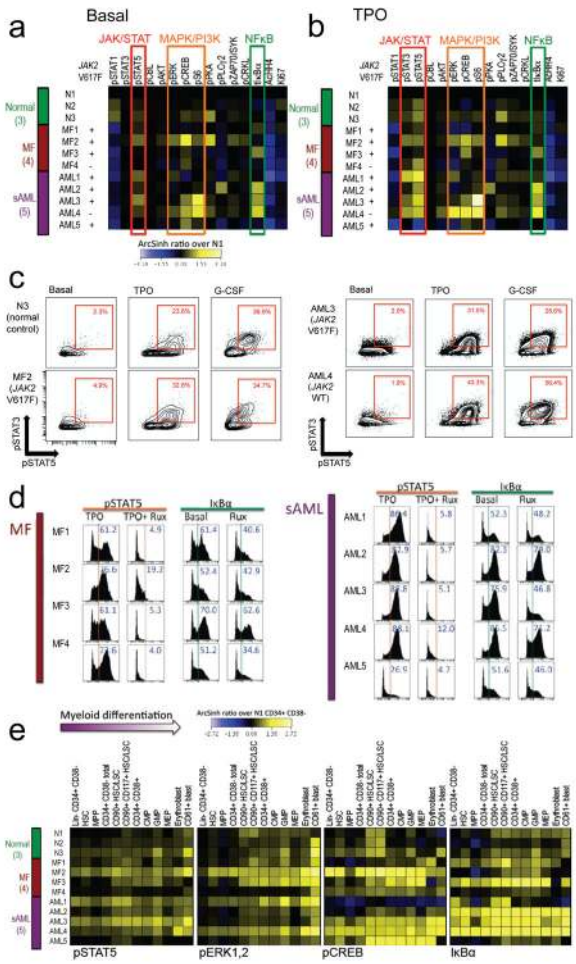

Figure 1. Heightened levels of multiple signaling molecules in MF and sAML hematopoietic stem and progenitor (HSPC) populations

Data are shown from a screening experiment using samples from three healthy bone marrow donor controls, four MF patients, and five sAML patients. **a.** Multiple signaling readouts observed in total Lin− CD34+ populations (derived from gating shown in Supplementary Figure S2), in the basal unstimulated state. Heat map tile color represents the arcsinh ratio (inverse hyperbolic sine: see Bendall et al., 2011[4] of median signal intensity normalized to healthy control bone marrow N1 (top row). Top three rows are healthy control bone marrow CD34+ cells (left bar); below them are four MF and 5 sAML patient samples. Presence or absence of the *JAK2* V617F mutation for each patient is listed in the column immediately left of each heat map. Each column shows the readout for a signaling molecule listed above it. Median signal intensity in MF and sAML HSPC normalized to N1 control is indicated for pSTAT5 (red box), markers of MAP kinase or PI3 kinase pathways (orange box), or IκBα (green box). **b.** Heat map of signaling readouts observed in total Lin− CD34+ populations, similar to a, in the presence of TPO. The red box indicative of elevated JAK-STAT signals in patient cells versus normal controls is expanded to include pSTAT3 signal in response to TPO. **c.** Biaxial plots illustrating pSTAT3 on the Y axis and pSTAT5 on the X axis for the Lin-CD34+ cell population. Panels show a normal bone marrow control (N3, top left), a

JAK2 V617F mutant MF patient (MF2, bottom left), and two sAML patients (AML3 and AML4, right). Conditions are, from left to right: basal (unstimulated), TPO, G-CSF. Percent of cells denoted as positive for both pSTAT3 and pSTAT5 phosphorylation is indicated by the red box with percentage shown. **d.** Histograms of pSTAT5 with TPO +/− ruxolitinib (left columns), and IκBα basally and with ruxolitinib (right columns), in MF and sAML CD34+ cells. Percentage value shown quantifies the percent of cells whose pSTAT5 or total IκBα signal intensity was considered unambiguously positive (vertical lines show gating). **e** Heat maps showing median basal levels of (maps displayed left to right) pSTAT5, pERK, pCREB, and total IκBα in HSPC subpopulations across a continuum of early myeloid development. Median values are displayed as arcsinh ratios normalized to the Lin− CD34+ CD38− population in the N1 healthy control. Gating for HSPC subpopulations is shown in Supplementary Figure S4.

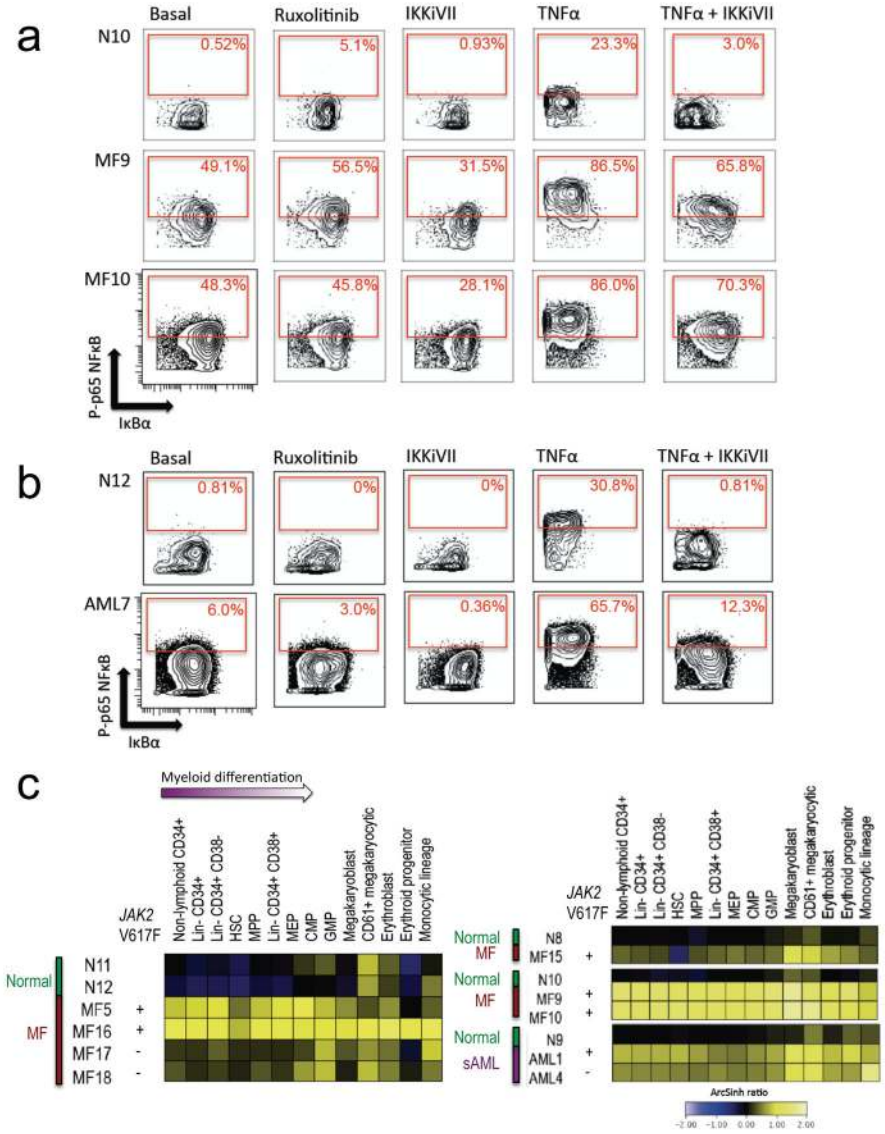

Figure 2. Elevation of basal and TNFα stimulated NFκB in MF and sAML

a. Biaxial plots showing phosphorylated p65/RELA NFκB versus total IκBα for the Lin−CD34+ population from a normal control (N10) and two MF patients (MF9 and MF10). Signals observed are shown in the basal state, and with treatment *ex vivo* with IKK inhibitor VII or TNFα, or with ruxolitinib. Percent in red box is the percent of cells with p-p65/RELA above >99% of the normal control distribution in the basal state. **b.** Biaxial plots similar to those in **a** for the Lin−CD34+ population from a normal control (N12) and an sAML patient (AML7). **c.** Heatmaps showing median basal p-p65/RELA within gated cell populations representing myeloid differentiation from immunophenotypic HSC to myeloid cells (gating in Supplementary Figure S4). Left, two normal controls and four MF patients, with values normalized to the N11 control non-lymphoid CD34+ population median. Right, independent experimental runs showing in total three MF and two sAML patients, with values normalized to the total non-lymphoid CD34+ cell median for each run-matched normal

control. Presence or absence of the *JAK2* V617F mutation for each patient is listed in the column immediately left of each heat map.

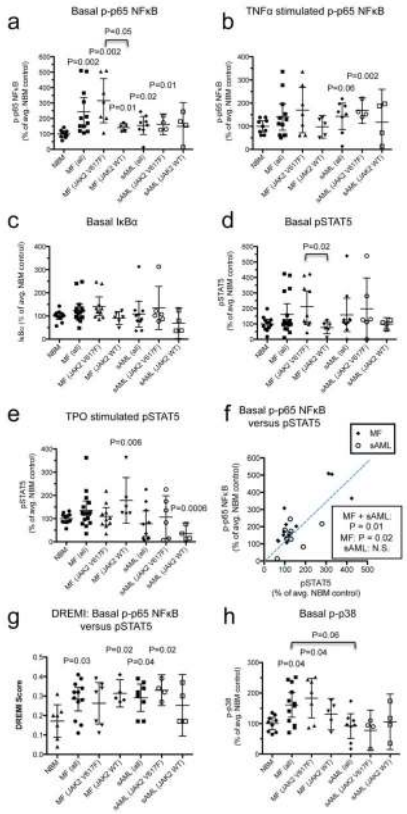

Figure 3. NFκB hyperactivation is frequent in MF and sAML

Statistical analysis of intracellular signaling in MF and sAML Lin−CD34+ cells compared with normal bone marrow (NBM) controls. **a–e** and **h:** Median levels of individual signaling markers are graphed for Lin−CD34+ cells from NBM, MF, and sAML (both total and grouped by *JAK2* genotype), and normalized to the mean among medians of NBM samples in each individual experiment (% of average control). **a.** Median basal p-p65/RELA levels for Lin−CD34+ cells from NBM, MF, and sAML. **b.** Median TNFα-induced p-p65/RELA levels. **c.** Median basal total IκBα levels. **d.** Median basal pSTAT5 levels. **e.** Median TPO-stimulated pSTAT5 levels. **f.** Paired median pSTAT5 and p-p65/RELA values from MF and sAML patients. **g.** DREMI analysis values for correlation of individual cell measurements of TPO-stimulated pSTAT5 and p-p65/RELA in the Lin−CD34+ cell population of patients and normal controls, where an elevated DREMI score indicates greater correlation of single cell pSTAT5 and p-p65/RELA measurements within the population. **h.** Median basal p-p38 levels in Lin−CD34+ cells. Error bars in **a–e** and **g–h** = mean +/− 95%CI. P values in column graphs represent deviation of distributions from the NBM distribution (excepting where indicated by brackets), calculated by Mann-Whitney U test, and listed for all sets where P ≤0.06. P values in f were calculated by Spearman r test for linear correlation.

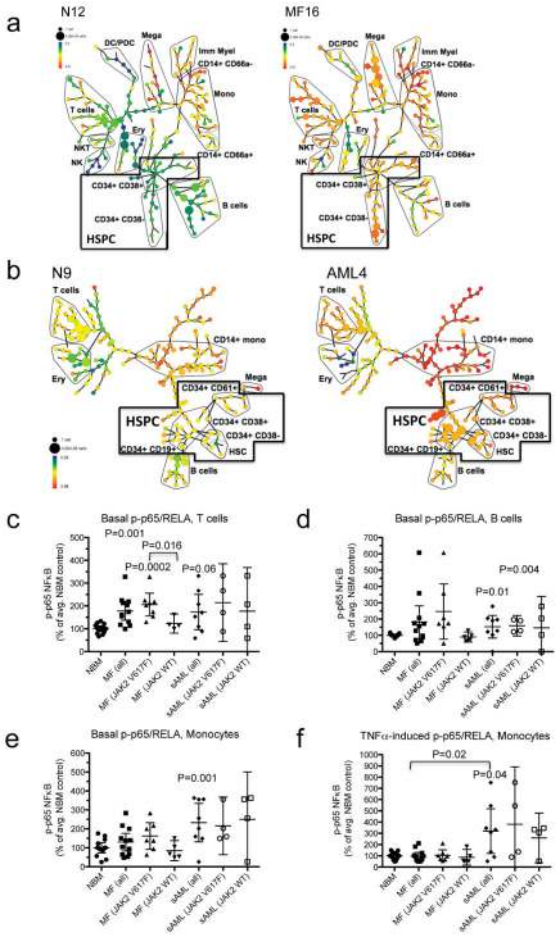

Figure 4. Cellular distribution of basally elevated p-65/RELA

a, b: SPADE dendrograms showing distributions and intensity of labeling for p-p65/RELA in the basal state. Basal median values (dual counts) of antibody labeling for each nodal cell population are denoted on color scale, with labeled cell clusters identified based on surface marker labeling. Color scales are blue/lowest to red/highest. CD34+ HSPC populations are indicated by thick outlined box in each diagram. **a.** p-p65/RELA levels, comparing a normal control bone marrow sample (N12) with an MF peripheral blood sample (MF16). **b.** p-p65/RELA levels, comparing a normal control bone marrow sample (N9) with an sAML peripheral blood sample (AML4). Abbreviations of identified cell populations: HSC, hematopoietic stem cells; HSPC, hematopoietic stem and progenitor cells; DC/PDC, dendritic and plasmacytoid dendritic cells; Mono, monocytes; Mega, megakaryocytic lineage cells; Imm myel, immature myeloid lineage cells; Ery, erythroid lineage cells; CD66a+, presumed maturing granulocytic lineage cells. Distinct SPADE tree shapes (**a** versus **b**) are indicative of separate experiments. **c.** Median basal p-p65/RELA levels in T cells from MF and sAML patients and normal controls. **d.** Median basal p-p65/RELA levels in B cells. **e.** Median basal p-p65/RELA levels in CD14+ monocytes**. f.** Median p-p65/RELA levels in monocytes in the presence of TNFα. Error bars in **c–f** = mean +/− 95%CI. P values represent deviation of distributions from the NBM distribution (excepting where

indicated by brackets), calculated by Mann-Whitney U test, and listed for all sets where $P \leq 0.06$.

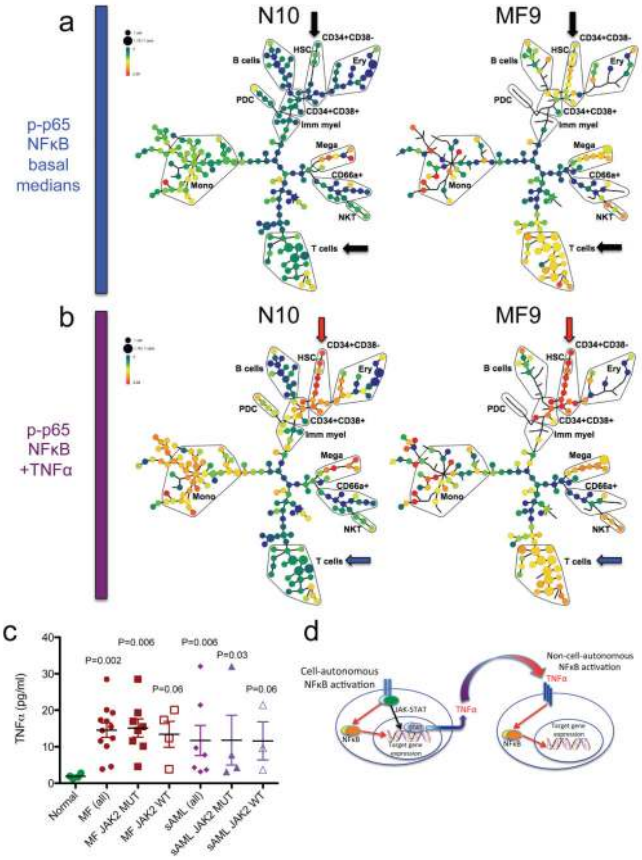

Figure 5. Cellular distribution of basal and TNFα-stimulated NFκB

SPADE dendrograms illustrating cell populations in whole bone marrow from a normal control (N10), and peripheral blood from an MF patient (MF9). **a,** Basal median values of p-p65/RELA for each nodal cell population, in dual counts on color scale, with labeled cell clusters identified based on surface marker labeling. Color scales are blue/lowest to red/highest. Elevated p-p65/RELA is evident in MF9 (above levels in N10) in CD34+ HSPC and in T cells (arrows). **b.** Median values of p-p65/RELA for each nodal cell population in the presence of TNFα. Levels of p-p65 RELA are elevated above those observed in the basal state in CD34+ HSPC (red arrows) but not in T cells (blue arrows). Abbreviations of identified cell populations: HSC, hematopoietic stem cells; HSPC, hematopoietic stem and progenitor cells; PDC, dendritic and plasmacytoid dendritic cells; Mono, monocytes; Mega, megakaryocytic lineage cells; Imm myel, immature myeloid lineage cells; Ery, erythroid lineage cells; CD66a+, presumed maturing granulocytic lineage cells. **c.** Plasma TNFα levels for MF and sAML patients from this study from whom peripheral blood plasma samples could be obtained, compared with healthy control plasma. P values (MF/sAML versus normal) were determined by Mann-Whitney U-test. Error bars = mean +/− SEM. **d.** Schematic of potential cell-autonomous and non-cell-autonomous mechanisms for NFκB activation resulting from JAK2 kinase hyperactivity.

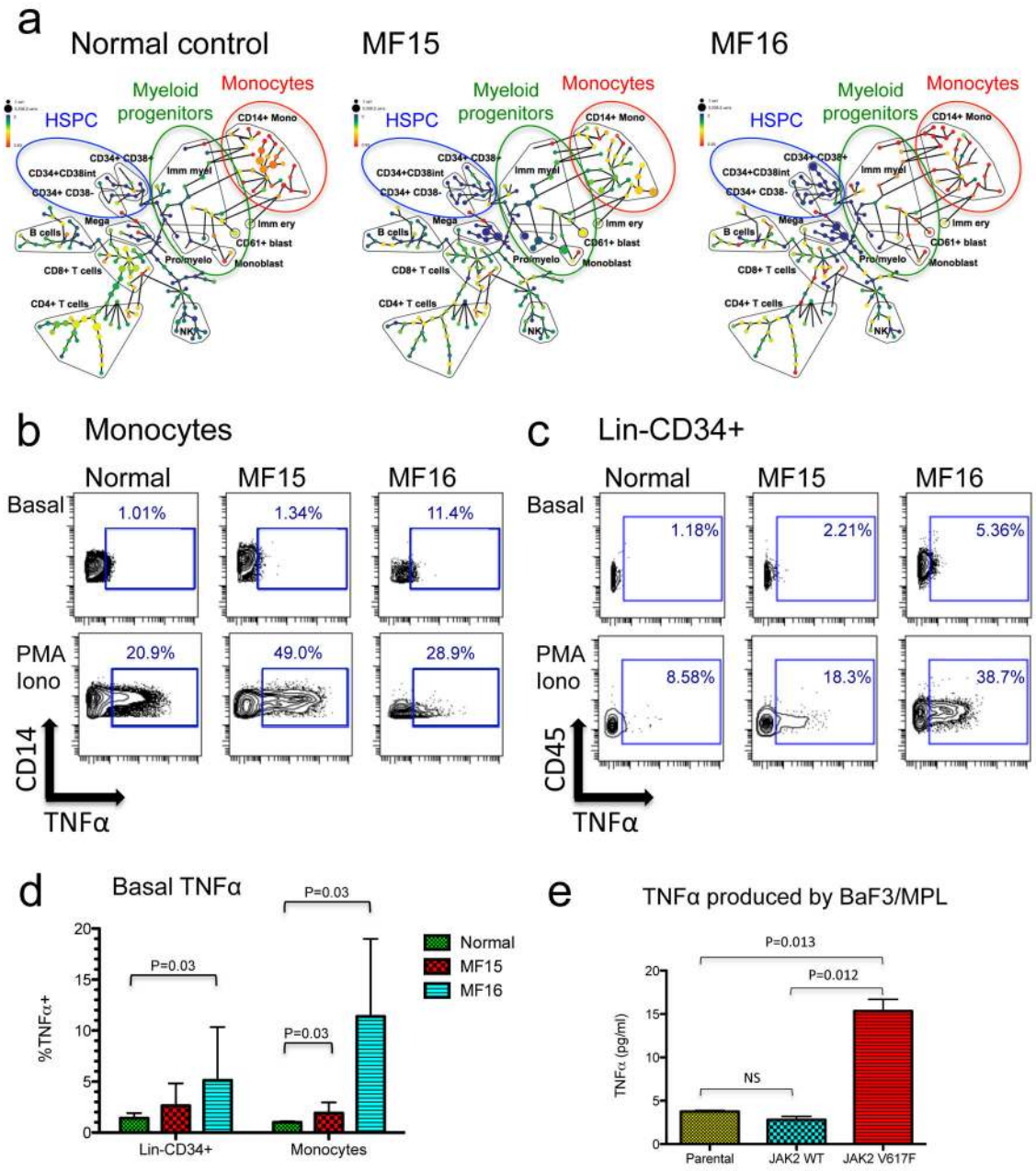

Figure 6. Elevated TNFα expression in MF myeloid cell populations

a. SPADE analysis illustrating location of intracellular TNFα in cell populations from normal peripheral blood control and two MF patients (MF15 and MF16) with observed elevated basal p-p65/RELA (see Figure 2, 4). The basal (unstimulated) condition is shown. Red in color scale indicates highest levels of TNFα. HSPC, myeloid progenitors, and monocytes are labeled by blue, green, and red ellipses, respectively. **b** and **c.** Biaxial plots showing intracellular TNFα in monocytes **(b)** and Lin−CD34+ cells **(c)** from normal peripheral blood control and two MF patients (MF15 and MF16). Plots show the basal (unstimulated) condition (top row), simulation with PMA + ionomycin (bottom row). Cell stimulations were of 4 hours duration in vitro. **d.** Bar graph of basal TNFα expression in Lin

–CD34+ cells and monocytes, showing percent of cells identified as positive for TNFα. Bars show mean + 95%CI for four independent experiments. P values shown where significant were derived by Mann-Whitney U test. **e.** TNFα yields from supernatants of Baf3/MPL cell line retrovirally expressing parental empty vector, wild-type *JAK2* virus, and *JAK2* V617F. Bars show mean plus range of duplicate measurements. P values were derived from 1-tailed T test.

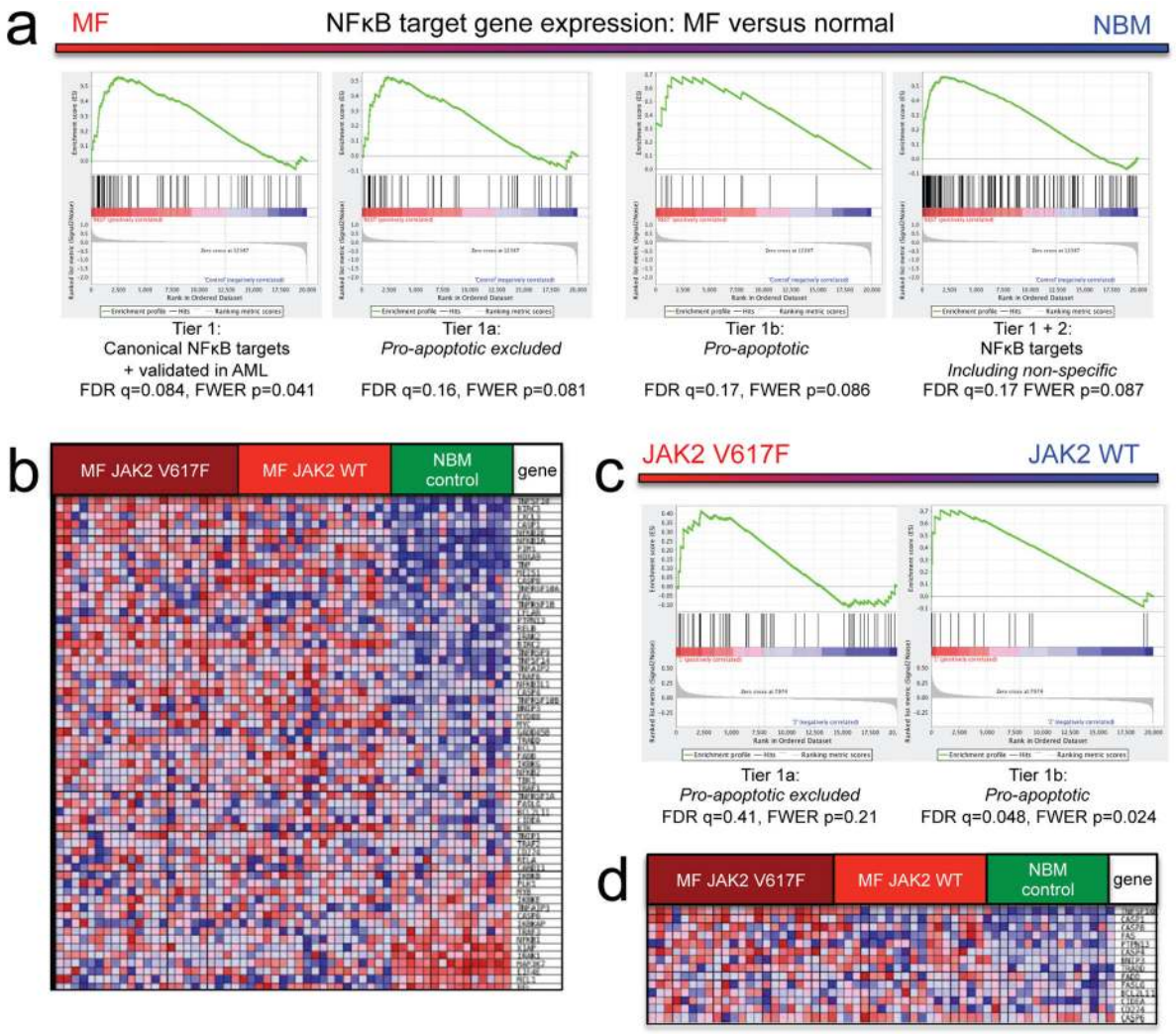

Figure 7. Increased NFκB pathway target gene expression in MF

a. Gene enrichment plots showing relative expression levels in MF versus normal control CD34+ cells. Left to right: Tier 1 (canonical and AML-related NFκB target genes); Tier 1a (canonical and AML-validated NFκB target genes, excluding pro-apoptotic genes); Tier 1b (pro-apoptotic NFκB target genes); Tier 1+2 (known NFκB target genes, including target genes shared with other signaling pathways), FDR q and FWER p values for each gene set are shown. Gene lists are in Supplementary Table S5. Gene expression datasets were previously published by Norfo et al.[40] **b.** Heat map showing higher gene expression in MF versus normal CD34+ cells (red) or lower expression in MF (blue) for the Tier 1 NFκB target gene list, using gene expression data from Norfo et al.[40] **c.** Gene enrichment plots showing relative expression levels in *JAK2* V617F versus *JAK2* wild-type MF patients. Tier 1a (canonical and AML-validated, pro-apoptotic excluded, left) and Tier 1b (pro-apoptotic, right) NFκB target gene sets are shown. **d.** Heat map for the pro-apoptotic Tier 1b gene set.

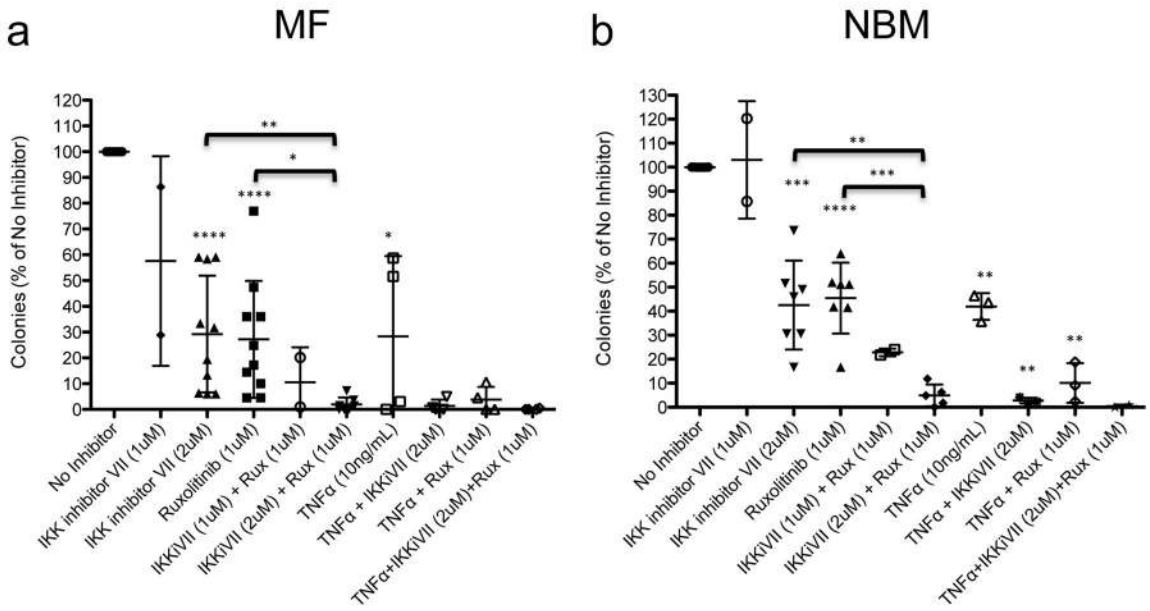

Figure 8. NFκB pathway inhibitors act in concert with ruxolitinib and TNFα to inhibit myeloid colony growth *in vitro*

Myeloid colonies derived from MF peripheral blood **(a)** and normal bone marrow **(b)** CD34+ cells, grown in the presence of one or more of ruxolitinib, IKKiVII, and TNFα, compared to no inhibitor and vehicle controls. Indicators of statistical significance over individual columns are compared to no inhibitor condition for inhibitors in absence of TNFα, and for TNFα alone; and to TNFα alone for inhibitors in the presence of TNFα. Error bars = mean =/− SD. Brackets indicate statistical significance over other paired conditions, if present. Statistical significance (determined by two-tailed T test): *, $p<0.05$; **, $p<0.01$; ***, $p<0.001$; ****, $p<0.0001$.